

# The pathogen protein EspF<sub>U</sub> hijacks actin polymerization using mimicry and multivalency

Nathan A. Sallee<sup>1,2</sup>, Gonzalo M. Rivera<sup>3</sup>, John E. Dueber<sup>2,†</sup>, Dan Vasilescu<sup>3</sup>, R. Dyché Mullins<sup>2</sup>, Bruce J. Mayer<sup>3</sup> & Wendell A. Lim<sup>2</sup>

Enterohaemorrhagic *Escherichia coli* attaches to the intestine through actin pedestals that are formed when the bacterium injects its protein EspF<sub>U</sub> (also known as TccP) into host cells<sup>1</sup>. EspF<sub>U</sub> potently activates the host WASP (Wiskott–Aldrich syndrome protein) family of actin-nucleating factors, which are normally activated by the GTPase CDC42, among other signalling molecules. Apart from its amino-terminal type III secretion signal, EspF<sub>U</sub> consists of five-and-a-half 47-amino-acid repeats. Here we show that a 17-residue motif within this EspF<sub>U</sub> repeat is sufficient for interaction with N-WASP (also known as WASL). Unlike most pathogen proteins that interface with the cytoskeletal machinery, this motif does not mimic natural upstream activators: instead of mimicking an activated state of CDC42, EspF<sub>U</sub> mimics an autoinhibitory element found within N-WASP. Thus, EspF<sub>U</sub> activates N-WASP by competitively disrupting the autoinhibited state. By mimicking an internal regulatory element and not the natural activator, EspF<sub>U</sub> selectively activates only a precise subset of CDC42-activated processes. Although one repeat is able to stimulate actin polymerization, we show that multiple-repeat fragments have notably increased potency. The activities of these EspF<sub>U</sub> fragments correlate with their ability to coordinate activation of at least two N-WASP proteins. Thus, this pathogen has used a simple autoinhibitory fragment as a component to build a highly effective actin polymerization machine.

Many pathogens target the cytoskeletal machinery of their host to facilitate attachment, entry or cell-to-cell spreading<sup>2,3</sup>. Enterohaemorrhagic *E. coli* (EHEC, O157:H7) causes severe gastrointestinal disease, and infection is dependent on attachment of the bacterium to intestinal epithelial cells by means of actin pedestals<sup>1</sup>. Pedestal formation is mediated by the pathogenic protein EspF<sub>U</sub> (*E. coli*-secreted protein F-like protein from prophage U; refs 4, 5), which is injected through a type III secretion system<sup>6</sup> into host cells where it stimulates actin polymerization by activating host WASP family proteins (Fig. 1a). WASPs are activators of the actin-related protein (ARP)2/3 complex, but under basal conditions this function is regulated by an autoinhibitory interaction between the GTPase-binding domain (GBD) and the ‘C-helix’ in the catalytic WCA region (named for its WASP-homology 2 (WH2) motif(s), C-helix, and acidic motif)<sup>7</sup>. Normal activation of N-WASP requires disruption of autoinhibition (Fig. 1b), involving the coordinated action of multiple endogenous activators, including CDC42, the phospholipid PtdIns(4,5)P<sub>2</sub>, and SH3-domain-containing proteins such as NCK (refs 8, 9; Fig. 1c). EspF<sub>U</sub> can independently activate N-WASP with a potency that is orders of magnitude higher than single endogenous activators<sup>8</sup> (Fig. 1c, d and Supplementary Fig. 1).

A common strategy exploited by pathogens in targeting host cell processes is to produce a protein that mimics an endogenous activator of that process<sup>6,10,11</sup>. This mimic will generally be constitutively active compared to the endogenous protein, which shows regulated activity<sup>12,13</sup>. Among pathogens that target actin polymerization, there

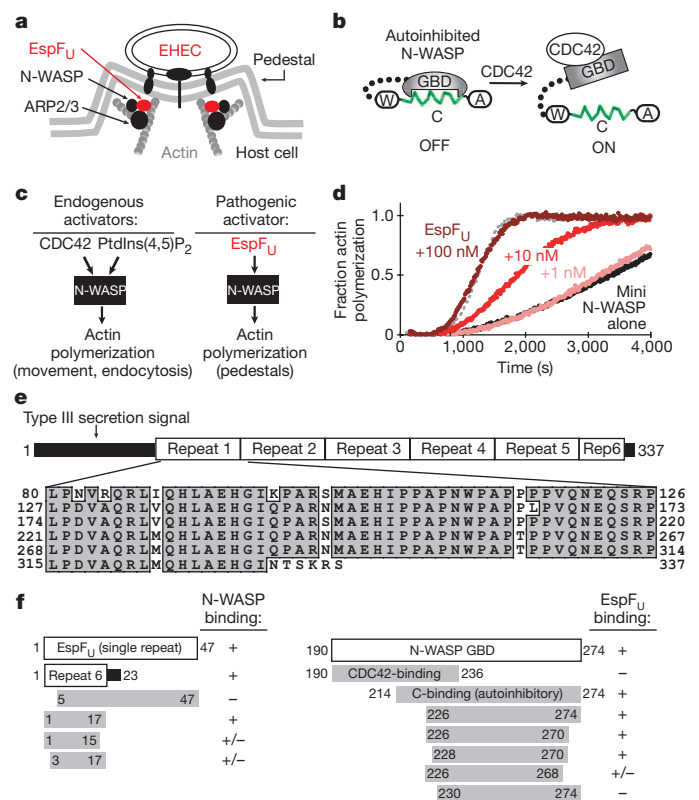


**Figure 1 | EspF<sub>U</sub> is a potent activator of N-WASP.** **a**, EspF<sub>U</sub> is secreted from EHEC into a host cell where it stimulates actin polymerization through endogenous N-WASP and ARP2/3, leading to pedestal formation. **b**, N-WASP is basally autoinhibited, but can be activated by inputs such as CDC42. **c**, Multiple endogenous activators are necessary to potently activate N-WASP. EspF<sub>U</sub> accomplishes this with a single input. **d**, EspF<sub>U</sub> potently activates N-WASP in an *in vitro* pyrene-actin-polymerization assay. Maximal rate (50 nM unregulated N-WASP WCA) is shown by the grey dotted line. All other reactions contain 50 nM mini N-WASP (GBD-linker-WCA). **e**, Sequence of EspF<sub>U</sub>. **f**, Mapping minimal binding fragments of EspF<sub>U</sub> and N-WASP with a GST-pull-down assay.

<sup>1</sup>Graduate Program in Chemistry and Chemical Biology and <sup>2</sup>Department of Cellular and Molecular Pharmacology and the Cell Propulsion Laboratory (an NIH Nanomedicine Development Center), University of California, San Francisco, 600 16th Street, San Francisco, California 94158, USA. <sup>3</sup>Raymond and Beverly Sackler Laboratory of Genetics and Molecular Medicine, Department of Genetics and Developmental Biology and Center for Cell Analysis and Modeling (CCAM), University of Connecticut Health Center, Farmington, Connecticut 06030, USA. †Present address: Department of Synthetic Biology, California Institute of Quantitative Biomedical Research (QB3), University of California, Berkeley, 327 Stanley Hall, Berkeley, California 94720, USA.

are examples of effector proteins that mimic the active states of N-WASP (ref. 14) or N-WASP activators such as CDC42 (ref. 15). Previous studies have shown that EspF<sub>U</sub> interacts with the GBD (refs 16, 17), the regulatory domain in N-WASP that participates in auto-inhibition and binds to activated CDC42 (ref. 7). Thus, we set out to test the hypothesis that EspF<sub>U</sub> may mimic an activated state of CDC42.

EspF<sub>U</sub> has a type III secretion signal followed by five-and-a-half 47-amino-acid repeats (Fig. 1e; a six-and-a-half-repeat isoform of EspF<sub>U</sub> has also been reported<sup>5</sup>). The repeats are nearly identical and share little sequence homology with other proteins, except for the related EHEC protein EspF. EspF also activates N-WASP (ref. 18) but does not participate in pedestal formation<sup>4,19</sup> (EspF contributes to the disruption of epithelial tight junctions).

We first mapped the minimal interacting fragments of both EspF<sub>U</sub> and N-WASP using pull-down-binding assays. We found that the N-WASP GBD could bind to a single EspF<sub>U</sub> repeat. We tested other truncations and found that the first 17 amino acids of each repeat constitute the minimal fragment with high affinity for the GBD (Fig. 1f and Supplementary Fig. 2). This sequence corresponds to a predicted  $\alpha$ -helix<sup>20</sup> and it is repeated six times in the full-length protein. There are minor sequence differences among the six copies of this motif, but the repeats seem to be equivalent in binding and functional assays (data not shown).

The N-WASP GBD is a composite regulatory domain made up of two overlapping elements—a CDC42-binding element and an auto-inhibitory element that binds to the C-helix<sup>7</sup>. Detailed mapping of the N-WASP side of the interaction showed that the carboxy-terminal, autoinhibitory portion of the GBD interacts with EspF<sub>U</sub> and that the amino-terminal, CDC42-binding portion does not. The minimal EspF<sub>U</sub>-binding fragment of N-WASP is residues 228–270 (Fig. 1f and Supplementary Fig. 2), which form the core of the interaction with the C-helix in the autoinhibited structure (Fig. 2a)<sup>7</sup>.

Because a small peptide from EspF<sub>U</sub> interacts with the autoinhibitory portion of the GBD, it seemed unlikely that EspF<sub>U</sub> was activating N-WASP by mimicking CDC42. Instead, we postulated that this EspF<sub>U</sub> fragment might be mimicking the C-helix and disrupting N-WASP autoinhibition by competitively binding to the GBD. We found that EspF<sub>U</sub> does indeed competitively disrupt the N-WASP autoinhibitory interaction in a pull-down-binding assay (Fig. 2b). Sequence alignment of the C-helix and the first 17 amino acids of the EspF<sub>U</sub> repeat revealed sequence homology at three positions at which hydrophobic amino acids are known to be critical for interaction with the GBD (Fig. 2a, c)<sup>21</sup>. We carried out a systematic alanine scan of both the N-WASP and the EspF<sub>U</sub> fragments and tested binding of the mutants to the GBD. The results showed that mutation of any of the conserved hydrophobic positions to alanine on either the C-helix or the EspF<sub>U</sub> fragment completely disrupted interaction with the GBD (Fig. 2c).

Previous work has shown that the isolated WASP GBD is only partially folded and unstable, but that fusion of the C-helix to the GBD leads to a stably folded, helical structure that approximates the autoinhibited state<sup>7</sup>. We made a fusion of the GBD to the minimal 17-amino-acid interacting fragment from EspF<sub>U</sub> and found that this protein had very similar helical content and thermal stability to the GBD–C-helix fusion (Supplementary Fig. 3).

These results show that the N-terminal 17 amino acids of the EspF<sub>U</sub> repeat are mimicking the C-helix (an autoinhibitory element) and this motif competitively disrupts autoinhibition of WASPs (Fig. 2d). A similar sequence motif is present in EspF and probably activates N-WASP using the same mechanism. We found that one EspF<sub>U</sub> repeat binds to the N-WASP GBD (amino acids 214–274) with a dissociation constant ( $K_d$ ) of 18 nM (Supplementary Fig. 4). This affinity is about 100-fold tighter than previously measured values for the corresponding WASP GBD–C-helix interaction (*in trans*)<sup>7</sup>, and this higher affinity explains how an intermolecular interaction can competitively disrupt an intramolecular interaction. The C-helix also

contributes to the interactions of N-WASP with actin monomers and the ARP2/3 complex<sup>22</sup>. We found that EspF<sub>U</sub> can bind to these molecules as well (Supplementary Fig. 4). In spite of this, EspF<sub>U</sub> cannot stimulate actin polymerization without N-WASP (data not shown).

Utilization of a competitive autoinhibitory fragment represents a previously unknown strategy for a pathogen to use in hijacking host cell signalling. One possible advantage of this strategy is increased specificity: a constitutively active signalling mimic will activate all downstream endogenous signalling pathways, whereas a mimic of a regulatory element should only activate a small subset. To test this idea, we investigated whether EspF<sub>U</sub> could activate the p21-activated kinases (PAKs)—another group of CDC42-responsive proteins, the regulation of which is most closely related to that of WASPs. CDC42 activates PAKs by disrupting an autoinhibitory interaction (which is structurally homologous to that of WASP)<sup>23</sup>. However, the PAK homologue of the WASP C-helix lacks the consensus sequence of three conserved hydrophobic amino acids. EspF<sub>U</sub> was unable to activate PAKs (Fig. 2e and Supplementary Fig. 5), indicating specificity of EspF<sub>U</sub> towards WASP family proteins (Fig. 2d). This more targeted activation may be advantageous for the pathogen, given the broad range of downstream effects mediated by WASP activators such as CDC42.

We also investigated the functional significance of this autoinhibitory mimic being repeated six times in one EspF<sub>U</sub> molecule. We tested the relative abilities of EspF<sub>U</sub> fragments of different lengths to stimulate actin assembly using an *in vitro* pyrene-actin-polymerization assay. One repeat from EspF<sub>U</sub> can disrupt the N-WASP autoinhibitory interaction in a binding assay (Supplementary Fig. 6), but has low ability to stimulate actin polymerization (comparable to that of a single endogenous activator; Fig. 3a). A fragment of two repeats

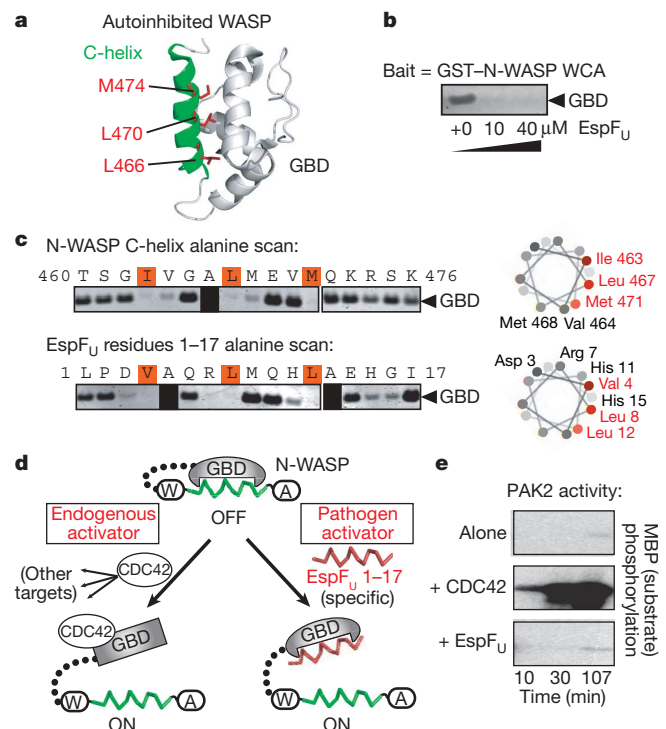


**Figure 2 | EspF<sub>U</sub> mimics the N-WASP autoinhibitory C-helix.** **a**, The structure of an autoinhibited fragment of WASP<sup>7</sup>, highlighting the C-helix (green) and three critical side chains (red). **b**, EspF<sub>U</sub> can competitively disrupt the N-WASP autoinhibitory interaction (*in trans*) in a GST-pull-down assay. **c**, Alanine scanning mutagenesis shows a similar pattern of critical residues in the N-WASP C-helix and in EspF<sub>U</sub> (repeat 4, residues 1–17; assayed by binding to GBD in a GST-pull-down assay). **d**, Model comparing N-WASP activation by CDC42 and EspF<sub>U</sub>. **e**, PAK kinase assay showing phosphorylation of myelin basic protein (MBP). PAK2 alone is autoinhibited; CDC42 activates it, but EspF<sub>U</sub> does not.

shows intermediate activity in the actin assay, but at least three repeats are necessary for high potency. Each additional repeat gives higher activity until full-length EspF<sub>U</sub> (residues 80–337, lacking the secretion signal), which has a maximal activity at the same level as unregulated N-WASP (Fig. 3a and Supplementary Fig. 7). To see whether this trend continued, we made an EspF<sub>U</sub> protein that has eight-and-a-half repeats and found that it reaches the same maximal activity as the wild-type protein, but is even more potent at low concentrations (Fig. 3a). At very high concentrations, EspF<sub>U</sub> proteins had a partial inhibitory effect on actin polymerization (data not shown), probably owing to EspF<sub>U</sub> sequestering actin monomers and/or ARP2/3.

We constructed a minimized EspF<sub>U</sub> protein in which six copies of the 17-residue C-helix mimic are separated by glycine–serine linkers. This construct was still able to stimulate actin polymerization (albeit with lower potency than wild-type EspF<sub>U</sub>), showing that the C-terminal portion of each EspF<sub>U</sub> repeat is not essential for activity (Supplementary Fig. 8).

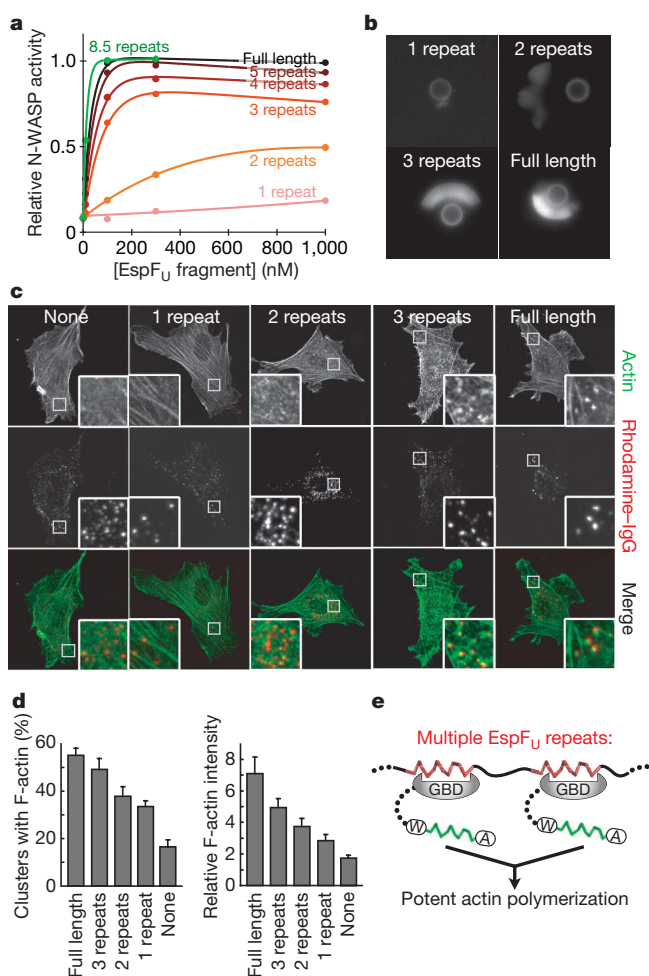


**Figure 3 | Multiple repeats of EspF<sub>U</sub> are required for potent activation of actin polymerization.** **a**, Activities of EspF<sub>U</sub> fragments in a pyrene-actin-polymerization assay. Data are fit to single exponential curves using Matlab (MathWorks), with a small linear term subtracted to account for EspF<sub>U</sub> sequestration of actin and/or ARP2/3. **b**, Visualization of fluorescently labelled actin around beads coated with EspF<sub>U</sub> fragments. Images were acquired four minutes after initiation. **c**, NIH 3T3 cells expressing GFP-actin and EspF<sub>U</sub> fused to a transmembrane protein (CD16/7), which is clustered with a rhodamine-tagged antibody<sup>26</sup>. Inset in each image is a portion of that cell (white box) shown at higher magnification. **d**, Results from quantification of clustered cells, shown in two metrics. Bars represent mean  $\pm$  s.e.m. of 10 cell images. **e**, Activity correlates with ability of EspF<sub>U</sub> fragments to bind at least two N-WASP proteins simultaneously.

Next, we tested whether multiple repeats were also required in more complex assays of actin assembly—namely a reconstituted bead motility assay and an *in vivo* clustering assay. In the first assay, EspF<sub>U</sub> fragments are chemically coupled to polystyrene beads; these beads are incubated with a mixture of actin and actin-regulatory proteins and are examined by microscopy for the ability to stimulate actin assembly and motility<sup>24</sup>. Beads coated with full-length EspF<sub>U</sub> triggered formation of an F-actin shell that breaks symmetry and induces transient polarized bead movement (Fig. 3b). Beads coated with three EspF<sub>U</sub> repeats showed similar behaviour (albeit with a slightly more diffuse actin shell), whereas two-repeat beads formed shells that were very diffuse, showed significantly reduced actin fluorescence, and disassembled within minutes. Beads coated with a single repeat showed minimal ability to polymerize actin (Fig. 3b). We varied the surface density of EspF<sub>U</sub> protein on the beads and found that this had little effect on the relative activities of the different fragments (data not shown). In particular, one-repeat beads had weak activity, even at maximal density. This shows that a high local concentration of a single repeat has minimal effect—multiple repeats in the same polypeptide chain are required for potent activation of actin polymerization.

To test the ability of EspF<sub>U</sub> fragments to form actin structures in cells, we used an antibody-induced clustering assay. Previous work has shown that N-WASP or N-WASP activators can form actin structures when clustered at the plasma membrane<sup>25</sup>. In our assay, the EspF<sub>U</sub> fragment was expressed as a fusion to the cytoplasmic tail of a transmembrane protein and then clustered using an antibody that recognizes the extracellular portion of the protein<sup>26</sup>. On clustering of full-length EspF<sub>U</sub>, we observed co-localization of N-WASP and bright actin foci to the clusters, showing that clustering of EspF<sub>U</sub> is sufficient to trigger localized actin assembly (Fig. 3c and Supplementary Figs 9 and 10). Furthermore, we tested three-, two- and one-repeat fragments and observed the same trend: three repeats showed similar activity to full-length EspF<sub>U</sub>, two repeats had intermediate activity and one repeat had lower activity (Fig. 3c). We used a computational image analysis tool (D.V., unpublished) to detect and correlate antibody and actin clusters (Supplementary Fig. 11). These quantitative results show that clustering of EspF<sub>U</sub> fragments with more repeats causes formation of actin clusters with higher frequency and intensity (Fig. 3d).

The requirement of multiple repeats for activation of actin polymerization suggests that EspF<sub>U</sub> needs to simultaneously bind and activate multiple N-WASP proteins to be highly active. To address this, we investigated the stoichiometry of the EspF<sub>U</sub>–N-WASP complex using analytical ultracentrifugation (AUC). By AUC (data not shown) and binding assays (Supplementary Fig. 12), we found that each repeat in an EspF<sub>U</sub> fragment could simultaneously bind an isolated N-WASP GBD (for example, a three-repeat fragment bound to three GBDs). However, the model in which EspF<sub>U</sub> has high potency because it can activate multiple N-WASPs does not explain why a two-repeat fragment has lowered activity in our actin assays. We found a likely answer to this question through stoichiometric analyses of complexes of a two-repeat protein with a larger, auto-inhibited N-WASP construct. These AUC data showed that whereas the two-repeat fragment can bind one N-WASP easily, binding of a second is less favourable (possibly owing to steric effects) and only happens in large excess of N-WASP (Supplementary Fig. 13). Larger fragments of EspF<sub>U</sub>, in contrast, readily formed complexes with two or more N-WASP proteins (Supplementary Fig. 13). Taken with our activation data, this suggests that activity of EspF<sub>U</sub> fragments correlates with their ability to coordinate the activation of at least two N-WASP proteins (Fig. 3e). There are a number of other cases in which oligomerization of WASPs or WASP activators leads to similarly increased activity—including the potent actin polymerization induced by glutathione *S*-transferase (GST)-tagged N-WASP WCA<sup>27</sup> (presumably owing to GST dimerization) and by oligomerized SNX9 in endocytosis<sup>28</sup>.

We have shown here that the EHEC protein EspF<sub>U</sub> has evolved a unique mechanism to potently and specifically activate N-WASP-mediated actin polymerization through a repeated autoinhibitory mimic. This co-opting of a small internal regulatory unit for activation of a target protein represents a previously unknown pathogenic strategy. Furthermore, multiple repeated copies of this motif are essential for potent activity, apparently because a single EspF<sub>U</sub> protein must coordinate simultaneous activation of multiple N-WASPs.

## METHODS SUMMARY

**EspF<sub>U</sub> expression and purification.** EspF<sub>U</sub> fragments were amplified by PCR from EHEC genomic DNA (ATCC). All cloning and expression was done in *E. coli* BLR(DE3) strains lacking recombinase A. Unless explicitly stated, EspF<sub>U</sub> fragments consist of the most N-terminal repeats.

**Pyrene-actin-polymerization assay.** ARP2/3 was purified from bovine brain, and actin was purified from rabbit muscle and pyrene-labelled, as described previously<sup>29</sup>. Actin polymerization was monitored as an increase in pyrene-actin fluorescence. Raw fluorescence data were normalized to the lower and upper baselines of each curve. Relative activities of EspF<sub>U</sub> fragments were determined through calculation of the time required to reach half-maximal fluorescence ( $t_{1/2}$ ).

**Bead motility assay.** Actin and ARP2/3 were purified from *Acanthamoeba castellanii*, as described previously<sup>30</sup>. EspF<sub>U</sub> proteins were coupled to polystyrene beads and mixed with actin, ARP2/3, N-WASP, capping protein and profilin. The assay was adapted from a protocol developed in ref. 24. Images were acquired with a Nikon TE300 Eclipse inverted epifluorescence microscope with constant imaging settings between experiments.

**In vivo clustering experiments.** NIH 3T3 fibroblasts were co-transfected with actin-GFP (green fluorescent protein) and the corresponding CD16/7 fusion construct. Cells were treated with clustering antibodies, as described previously<sup>26</sup>. Fixed cells were imaged with an oil-immersion  $\times 60$  NA 1.4 objective on a Zeiss LSM 510 Meta microscope. Imaging settings were constant between experiments, except for minor adjustments of detector gain to accommodate variation in expression level.

Quantitative detection of clusters was performed with a computational tool developed by D. Vasilescu. Ten cell images from three independent experiments were quantified for each construct. Data were presented in two metrics: the percentage of antibody clusters that have associated actin clusters and the intensities of these associated actin clusters. The relative intensity value is the ratio of the sum of intensities of associated actin clusters to the sum of intensities of all antibody clusters.

**Full Methods** and any associated references are available in the online version of the paper at [www.nature.com/nature](http://www.nature.com/nature).

Received 24 December 2007; accepted 12 June 2008.

Published online 23 July 2008.

- Caron, E. *et al.* Subversion of actin dynamics by EPEC and EHEC. *Curr. Opin. Microbiol.* **9**, 40–45 (2006).
- Gruenheid, S. & Finlay, B. B. Microbial pathogenesis and cytoskeletal function. *Nature* **422**, 775–781 (2003).
- Rottner, K., Lommel, S., Wehland, J. & Stradal, T. E. Pathogen-induced actin filament rearrangement in infectious diseases. *J. Pathol.* **204**, 396–406 (2004).
- Campellone, K. G., Robbins, D. & Leong, J. M. EspF<sub>U</sub> is a translocated EHEC effector that interacts with Tir and N-WASP and promotes Nck-independent actin assembly. *Dev. Cell* **7**, 217–228 (2004).
- Garmendia, J. *et al.* Tccp is an enterohaemorrhagic *Escherichia coli* O157:H7 type III effector protein that couples Tir to the actin-cytoskeleton. *Cell. Microbiol.* **6**, 1167–1183 (2004).
- Galan, J. E. & Wolf-Watz, H. Protein delivery into eukaryotic cells by type III secretion machines. *Nature* **444**, 567–573 (2006).
- Kim, A. S., Kakalis, L. T., Abdul-Manan, N., Liu, G. A. & Rosen, M. K. Autoinhibition and activation mechanisms of the Wiskott–Aldrich syndrome protein. *Nature* **404**, 151–158 (2000).
- Prehoda, K. E., Scott, J. A., Mullins, R. D. & Lim, W. A. Integration of multiple signals through cooperative regulation of the N-WASP–Arp2/3 complex. *Science* **290**, 801–806 (2000).

- Rohatgi, R., Nollau, P., Ho, H. Y., Kirschner, M. W. & Mayer, B. J. Nck and phosphatidylinositol 4,5-bisphosphate synergistically activate actin polymerization through the N-WASP–Arp2/3 pathway. *J. Biol. Chem.* **276**, 26448–26452 (2001).
- Mattoo, S., Lee, Y. M. & Dixon, J. E. Interactions of bacterial effector proteins with host proteins. *Curr. Opin. Immunol.* **19**, 392–401 (2007).
- Stebbins, C. E. Structural insights into bacterial modulation of the host cytoskeleton. *Curr. Opin. Struct. Biol.* **14**, 731–740 (2004).
- Mukherjee, S., Hao, Y. H. & Orth, K. A newly discovered post-translational modification — the acetylation of serine and threonine residues. *Trends Biochem. Sci.* **32**, 210–216 (2007).
- Aktories, K. & Barbieri, J. T. Bacterial cytotoxins: targeting eukaryotic switches. *Nature Rev. Microbiol.* **3**, 397–410 (2005).
- Zalavsky, J., Grigorova, I. & Mullins, R. D. Activation of the Arp2/3 complex by the *Listeria acta* protein. Acta binds two actin monomers and three subunits of the Arp2/3 complex. *J. Biol. Chem.* **276**, 3468–3475 (2001).
- Alto, N. M. *et al.* Identification of a bacterial type III effector family with G protein mimicry functions. *Cell* **124**, 133–145 (2006).
- Lommel, S., Benesch, S., Rohde, M., Wehland, J. & Rottner, K. Enterohaemorrhagic and enteropathogenic *Escherichia coli* use different mechanisms for actin pedestal formation that converge on N-WASP. *Cell. Microbiol.* **6**, 243–254 (2004).
- Garmendia, J., Carlier, M. F., Egile, C., Didry, D. & Frankel, G. Characterization of Tccp-mediated N-WASP activation during enterohaemorrhagic *Escherichia coli* infection. *Cell. Microbiol.* **8**, 1444–1455 (2006).
- Alto, N. M. *et al.* The type III effector EspF coordinates membrane trafficking by the spatiotemporal activation of two eukaryotic signaling pathways. *J. Cell Biol.* **178**, 1265–1278 (2007).
- McNamara, B. P. *et al.* Translocated EspF protein from enteropathogenic *Escherichia coli* disrupts host intestinal barrier function. *J. Clin. Invest.* **107**, 621–629 (2001).
- Rost, B., Yachdav, G. & Liu, J. The PredictProtein server. *Nucleic Acids Res.* **32**, W321–W326 (2004).
- Panchal, S. C., Kaiser, D. A., Torres, E., Pollard, T. D. & Rosen, M. K. A conserved amphipathic helix in WASP/Scar proteins is essential for activation of Arp2/3 complex. *Nature Struct. Biol.* **10**, 591–598 (2003).
- Marchand, J. B., Kaiser, D. A., Pollard, T. D. & Higgs, H. N. Interaction of WASP/Scar proteins with actin and vertebrate Arp2/3 complex. *Nature Cell Biol.* **3**, 76–82 (2001).
- Lei, M. *et al.* Structure of PAK1 in an autoinhibited conformation reveals a multistage activation switch. *Cell* **102**, 387–397 (2000).
- Akin, O. & Mullins, R. D. Capping protein increases the rate of actin-based motility by promoting filament nucleation by the Arp2/3 complex. *Cell* **133**, 841–851 (2008).
- Castellano, F. *et al.* Inducible recruitment of Cdc42 or WASP to a cell-surface receptor triggers actin polymerization and filopodium formation. *Curr. Biol.* **9**, 351–360 (1999).
- Rivera, G. M., Briceno, C. A., Takeshima, F., Snapper, S. B. & Mayer, B. J. Inducible clustering of membrane-targeted SH3 domains of the adaptor protein Nck triggers localized actin polymerization. *Curr. Biol.* **14**, 11–22 (2004).
- Higgs, H. N. & Pollard, T. D. Activation by Cdc42 and PIP(2) of Wiskott–Aldrich syndrome protein (WASP) stimulates actin nucleation by Arp2/3 complex. *J. Cell Biol.* **150**, 1311–1320 (2000).
- Yarar, D., Waterman-Storer, C. M. & Schmid, S. L. SNX9 couples actin assembly to phosphoinositide signals and is required for membrane remodeling during endocytosis. *Dev. Cell* **13**, 43–56 (2007).
- Sallee, N. A., Yeh, B. J. & Lim, W. A. Engineering modular protein interaction switches by sequence overlap. *J. Am. Chem. Soc.* **129**, 4606–4611 (2007).
- Dayel, M. J., Holleran, E. A. & Mullins, R. D. Arp2/3 complex requires hydrolyzable ATP for nucleation of new actin filaments. *Proc. Natl Acad. Sci. USA* **98**, 14871–14876 (2001).

**Supplementary Information** is linked to the online version of the paper at [www.nature.com/nature](http://www.nature.com/nature).

**Acknowledgements** We thank O. Akin for reagents and assistance with the bead motility experiments; J. C. Anderson, A. Chau, R. Howard, M. Lohse, A. Remenyi and L. Weaver for assistance; and members of the Lim laboratory for discussion. This work was supported by grants from the NIH (NIGMS and Nanomedicine Development Centers, NIH Roadmap), the NSF and the Packard Foundation. G.M.R. was supported by the American Heart Association.

**Author Information** Reprints and permissions information is available at [www.nature.com/reprints](http://www.nature.com/reprints). Correspondence and requests for materials should be addressed to W.A.L. ([lim@cmp.ucsf.edu](mailto:lim@cmp.ucsf.edu)).

## METHODS

**Protein construction and purification.** Because of the high DNA sequence conservation between EspF<sub>U</sub> repeats, PCR reactions would result in a ladder of bands on a gel that corresponded to 1 repeat, 2 repeats, and so on. We made repeat fragments by cutting out the bands that corresponded to 1 repeat up to 5 repeats. EspF<sub>U</sub> proteins were expressed as N-terminal hexahistidine (pET19-derived vector) or GST (pGEX4T-1 vector) fusions and purified on Ni-NTA resin (Qiagen) or glutathione agarose (Sigma), respectively. Proteins were further purified by ion exchange chromatography on a Source Q column (Pharmacia).

The synthetic eight-and-a-half-repeat EspF<sub>U</sub> protein was assembled through introduction of a silent AatII restriction site near the N terminus of the repeat. By PCR, we made one three-repeat fragment starting at the N terminus of EspF<sub>U</sub> and ending with the AatII site, and a second five-and-a-half-repeat fragment starting with the AatII site and ending at the C terminus of EspF<sub>U</sub>. These two fragments were cut with AatII (NEB) and ligated to form the eight-and-a-half-repeat protein.

The two WASP family proteins used in this study are human WASP (referred to as 'WASP') and rat neuronal WASP (referred to as 'N-WASP'). Mini N-WASP consists of residues 178–274 fused to residues 392–501 through a 9-amino-acid glycine-serine linker.

Single alanine mutations of the N-WASP C-helix (residues 452–487) and EspF<sub>U</sub> C-mimic (repeat 4, residues 1–17) sequences were made using QuikChange mutagenesis<sup>31</sup>. Mutants were expressed as GST fusions.

**GST-pull-down binding assays.** GST-tagged bait protein was bound to glutathione agarose. Sufficient resin was added to bring the bait protein concentration to 1 μM. Hexahistidine-tagged prey protein was added at 10 μM. For competitions, a series of pull-downs were performed with increasing concentration of the competitor. Binding was performed in 20 mM Tris, pH 8.0, 50 mM NaCl and 1 mM DTT. Bound prey protein was detected by western blotting with a mouse His-probe primary antibody (Santa Cruz Biotech), followed by a fluorescent goat anti-mouse IRDye 800CW secondary antibody (Li-Cor Biosciences). Bands were visualized on a Li-Cor Odyssey infrared fluorescence scanner.

**PAK kinase assays.** Assays were performed as described previously<sup>32</sup>. Human PAK1 and PAK2 proteins were purchased from Cell Signaling Technology. MBP (Invitrogen) from bovine brain was used as the phosphorylation substrate. The CDC42 used is a soluble fragment of the human protein (residues 1–179) bearing a G12V constitutively active mutation. Each reaction was performed with 0.5 μg PAK and 15 μg MBP substrate in 35 μl volume, with or without 2.5 μg of CDC42 G12V or full-length EspF<sub>U</sub>. The assay buffer consisted of 50 mM HEPES, pH 7.5, 10 mM MgCl<sub>2</sub>, 10 mM NaF, 2 mM MnCl<sub>2</sub>, 1 mM DTT and 0.05% Triton X-100. The reaction was initiated by addition of 10 μCi [ $\gamma$ -<sup>33</sup>P]ATP. Aliquots were removed at three time points. Samples were analysed by SDS-PAGE, vacuum dried and exposed to film.

**Pyrene-actin-polymerization assays.** Assays were performed essentially as described previously<sup>33</sup>. Exact assay conditions were 1.3 μM actin (10% pyrene-labelled), 20 nM ARP2/3, 50 nM mini N-WASP, 50 mM KCl, 1 mM MgSO<sub>4</sub>, 1 mM EGTA, 0.2 mM ATP, 1 mM DTT, 3 μM MgCl<sub>2</sub> and 11.5 mM imidazole, pH 7.0, in a total volume of 100 μl. Actin polymerization was monitored as an increase in pyrene-actin fluorescence (excitation: 365 nm; emission: 407 nm) with a SpectraMax Gemini XS fluorescence plate reader (Molecular Devices). Raw fluorescence data were normalized to the lower and upper baselines of each

curve using the equation  $(F_{\text{data}} - F_{\text{lower}})/(F_{\text{upper}} - F_{\text{lower}})$ . To determine the minimal (min) rate of actin polymerization, mini N-WASP was omitted from the assay (ARP2/3 alone) and to determine the maximal (max) rate, mini N-WASP was replaced by 50 nM unregulated N-WASP WCA. Relative activities of EspF<sub>U</sub> fragments were determined with the equation  $[t_{1/2}(\text{min}) - t_{1/2}(\text{data})]/[t_{1/2}(\text{min}) - t_{1/2}(\text{max})]$ .

**Bead motility assays.** Actin was labelled with rhodamine. Human profilin I (ref. 34) and mouse capping protein CP  $\alpha$ 1 $\beta$ 2 (ref. 35) were grown recombinantly and purified as described previously. GST fusions of EspF<sub>U</sub> fragments were covalently crosslinked to 5 μm carboxylated polystyrene beads (Bangs Labs). In brief, 1% (w/v) solutions of beads were charged with EDC and stabilizing SulfoNHS (Pierce) and then reacted with 4 μM of the GST-fused EspF<sub>U</sub> fragment. We also coupled EspF<sub>U</sub> fragments diluted in GST alone. Coupling reactions were quenched with Tris and the beads were washed to remove non-covalently attached protein. EspF<sub>U</sub>-coupled bead solutions were diluted 1:30 into a motility mixture consisting of 62.5 nM ARP2/3, 300 nM capping protein, 3 μM profilin and 100 nM  $\Delta$ EVH1 N-WASP (residues 136–501) in 0.5 mM ATP, 1 mM MgCl<sub>2</sub>, 1 mM EGTA, 15 mM TCEP, 50 mM KOH, 20 mM HEPES, pH 7.0, 2.5 mg ml<sup>-1</sup> BSA and 0.2% methylcellulose. Motility was initiated by addition of 7.5 μM actin (5% labelled). Samples were mounted between silanized glass slides and coverslips. Images in the paper are of beads coated with EspF<sub>U</sub> fragments diluted 1:4 in GST alone. We also tested beads with maximal surface density of EspF<sub>U</sub> fragments (no GST added) and observed the same trends in activity (data not shown).

**In vivo clustering assays and quantification.** Details of the CD16/7 chimaeric construct were described previously<sup>26</sup>. Aggregation of membrane-targeted EspF<sub>U</sub> fragments was performed by antibody-mediated cross-linking of CD16/7 (ref. 26). In brief, 24 h after transfection, cells were incubated with a mouse CD16 antibody (Calbiochem) at 1 μg ml<sup>-1</sup> in complete medium for 1 h at 37 °C. After washing, cells were incubated with rhodamine-conjugated goat anti-mouse IgG (Pierce) at 0.5 μg ml<sup>-1</sup> for an additional hour. Fluorescent images were collected on a Zeiss LSM 510 Meta confocal microscope using a  $\times$ 63 NA 1.4 Plan-NEOFLUAR oil immersion objective. Specimens were illuminated with an argon laser with emission at 488 nm and a HeNe laser with emission at 543 nm.

Quantitative data were derived using the Comet Detector, a newly developed computational tool (D.V., unpublished). For details, see the Supplementary Information.

- Wang, W. & Malcolm, B. A. Two-stage PCR protocol allowing introduction of multiple mutations, deletions and insertions using QuikChange Site-Directed Mutagenesis. *Biotechniques* **26**, 680–682 (1999).
- Chong, C., Tan, L., Lim, L. & Manser, E. The mechanism of PAK activation. Autophosphorylation events in both regulatory and kinase domains control activity. *J. Biol. Chem.* **276**, 17347–17353 (2001).
- Machesky, L. M. *et al.* Scar, a WASP-related protein, activates nucleation of actin filaments by the Arp2/3 complex. *Proc. Natl Acad. Sci. USA* **96**, 3739–3744 (1999).
- Kaiser, D. A., Goldschmidt-Clermont, P. J., Levine, B. A. & Pollard, T. D. Characterization of renatured profilin purified by urea elution from poly-L-proline agarose columns. *Cell Motil. Cytoskeleton* **14**, 251–262 (1989).
- Palmgren, S., Ojala, P. J., Wear, M. A., Cooper, J. A. & Lappalainen, P. Interactions with PIP2, ADP-actin monomers, and capping protein regulate the activity and localization of yeast twinfilin. *J. Cell Biol.* **155**, 251–260 (2001).